Asymmetric Curvature Side-Polished Optical Fiber Coupler

Takui Uematsu, Kazutaka Noto, Hiroyuki Iida, Chisato Fukai, and Ikutaro Ogushi

***Abstract*—An optical fiber coupler composed of two side-polished fibers with different curvature is proposed. The live-fiber is polished with a typical radius of curvature of 0.25 m, while the branch-fiber is polished with a larger radius of curvature. Analysis shows that the proposed asymmetric structure improves the highest cross-transmission of the coupled light by up to 0.26 just by increasing the curvature of the branch-fiber (compared to the conventional symmetric arrangement) without increasing the insertion loss created by side-polishing. Experiments confirm that the proposed structure raises the highest cross-transmission by 0.15 on average when the curvature of the branch-fiber is set to 0.5 m while the curvature of the live-fiber is kept to the typical value as expected from the analysis. Our study will contribute to realizing a simple and compact machine for polishing live-fibers that offers the improved workability and portability needed for adding optical fiber couplers to live-fibers in the field.**

***Index Terms*—Optical fiber coupler, side-polished fiber.**

I. Introduction

FIBER-TO-THE-HOME services have been established around the world by employing optical access networks (NWs) based on the tree-and-branch type passive optical architecture, such as gigabit passive optical network (G-PON) [1] and gigabit Ethernet PON (GE-PON) [2]. The tree-and-branch type architecture has the advantage of being able to efficiently accommodate subscribers in residential areas and business districts with high population densities. However, a bus-type optical access NW has been proposed for efficiently accommodating subscribers scattered over wide areas such as the countryside [3], [4], [5], [6]. In the bus-type NW, multiple branch fibers are connected to a single trunk fiber by installing optical couplers, so the coupler is an important component. Conventional optical couplers are inserted by cutting and terminating the trunk fiber, which interrupts FTTH services. One solution to avoid the service interruption is to install in advance more couplers than initially needed when constructing the NW to meet future demand forecasts. However, the installation of more couplers than necessary degrades the loss budget, which reduces the reach of the NW and the number of accommodated subscribers, due to the insertion loss of each coupler, or the power extracted by each coupler. In order to insert the coupler to the trunk fiber as needed without service interruption, an optical coupler insertion technique based on side-polished fibers has been proposed [7]. This technique side-polishes the live-fiber to achieve low insertion loss and high cross-transmission (up to 0.95) of the coupled light.

Side-polished fibers are usually fabricated by the V-groove assisted polishing technique [7], [8], [9], [10], [11], [12], [13], [14] or by the wheel polishing technique [15], [16], [17]. In the V-groove assisted polishing technique, side-polished fibers are achieved while holding the fiber in a V-groove with radius of curvature of R cut into a glass block. V-groove assisted technique is often used in side-polished fiber coupler fabrication where cross-transmission adjustment is required, because the polished fiber is protected by the V-groove. Side-polished fibers with various R values have been reported so far. R of 0.25 m is a typical choice [10], [11] and commercial polishers are available. This is because it is relatively easy to fabricate and the interaction length required for full-coupling can be obtained. However, larger R values such as 1 and 2.5 m have been shown to yield longer interaction lengths [7], [12], [14]. Increasing R expands the interaction length of the curved fiber coupler, which lowers the insertion loss created by polishing to 0.14 dB while raising the cross-transmission to 0.95 [7]. Unfortunately, larger R values need more precise and larger polishing machines because the length of the polished surface increases in proportion to the square root of R. The side-polishing of a live-fiber must be performed in narrow spaces such as aerial or underground closures, and so simple and compact polishing techniques are desirable to improve workability and portability. Thus, a side-polished fiber coupler that achieves high cross-transmission with smaller R value of the live-fiber is required.

In this paper, in order to reduce the radius of curvature of the live-fiber while maintaining the desired insertion loss and cross-transmission, an optical fiber coupler that consists of two side-polished fibers with different curvature is proposed. The asymmetric structure consisting of a multimode fiber and a double clad fiber has already been researched to achieve an efficient pumping of power lasers [18], [19]. We propose the asymmetric single-mode optical fiber coupler and introduce equations that simplify the calculation of the cross- and through- transmission in designing the radii of curvature of the asymmetric coupler. A theoretical study verifies that the proposed asymmetric structure improves cross-transmission by up to 0.26 without narrowing the core spacing, i.e., increasing the insertion loss by the polishing, compared to the conventional symmetric one. In experiments,

Manuscript received 29 April 2023; revised 23 June 2023; accepted 5 July 2023. Date of publication 10 July 2023; date of current version 17 July 2023. *(Corresponding author: Takui Uematsu.)*

The authors are with the Access Network Service Systems Laboratories, Nippon Telegraph and Telephone Corporation, Tsukuba, Ibaraki 305-0805, Japan (e-mail: takui.uematsu@ntt.com; kazutaka.noto@ntt.com; hiroyuki.iida@ntt.com; chisato.fukai@ntt.com; ikutaro.oogushi@ntt.com).

Digital Object Identifier 10.1109/JPHOT.2023.3293657

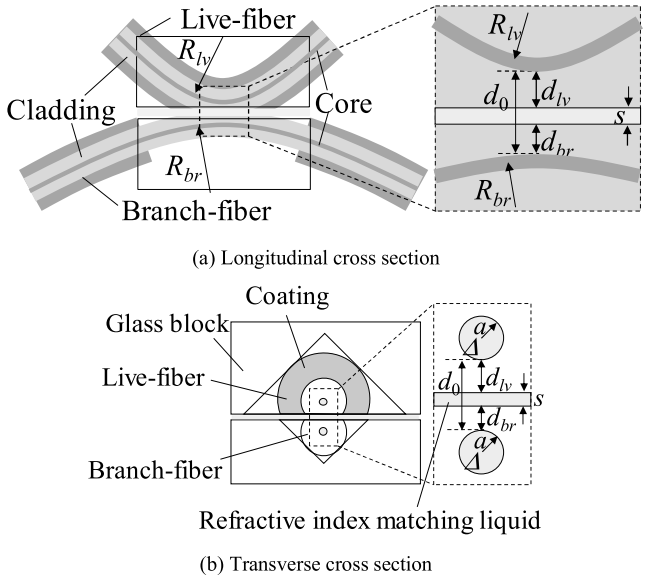

(a) Longitudinal cross section

(b) Transverse cross section

Fig. 1. Structure of the proposed side-polished fiber coupler with asymmetric curvature.

we fabricate side-polished live-fibers with the typical curvature value of 0.25 m, and side-polished branch-fibers with curvature of 0.25 and 0.5 m to compare the asymmetric structure with the symmetric one. Experimental results show that the proposed structure raises the highest cross-transmission by 0.15 on average without increasing the insertion loss. Our study will contribute to realizing the side-polishing of live-fibers with simple and compact polishing machines which will significantly enhance practicality.

II. Proposed Asymmetric Curvature Side-Polished Fiber Coupler

Fig. 1 shows the structure of the proposed side-polished fiber coupler. Live- and branch-fibers are identical single mode fibers compliant with ITU-T G. 652; they have core radius a and relative refractive index difference Δ. The branch-fiber is fabricated in a factory or elsewhere in advance as a stripped fiber with diameter of 0.125 mm. The live-fiber, which is polished in the field, is a coated fiber with diameter of 0.25 mm to avoid stripping which normally demands careful work and degrades the efficiency of field work. R_{lv} and R_{br} are the radii of curvature of the live- and branch-fibers, respectively. d_{lv} and d_{br} are the shortest distances between the polished surface and the core of the live- and branch- fibers, respectively, called remaining cladding thickness (RCT). s is the spacing between the polished surfaces of the live- and branch- fibers, and is mainly caused by unevenness of the polished surface. The space is filled with refractive index matching liquid to avoid any reflection at the polished surfaces. d_0 is the top-to-top core distance between the live- and branch- fibers, and is given by $d_0 = d_{lv} + d_{br} + s$. The geometry of the proposed side-polished fiber coupler is illustrated in Fig. 2. Using a parabolic approximation, $h(z)$, the center-to-center spacing between fibers at position z, can be

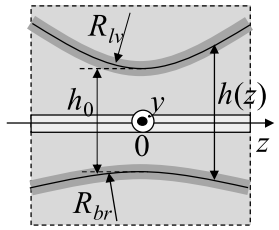

Fig. 2. Geometry of the proposed side-polished fiber coupler. Z-axis origin is at the position of minimum core-to-core spacing.

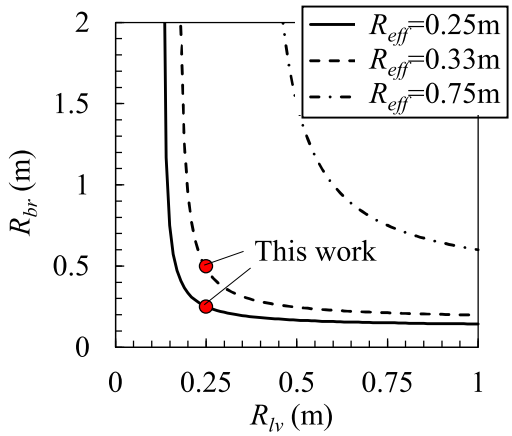

Fig. 3. R_{eff} as a function of R_{lv} and R_{br}. In our experiment, we chose $R_{lv} = 0.25$ m, $R_{br} = 0.25$ and 0.5 m.

expressed as

$$h(z) = \sqrt{\left(h_0 + \frac{z^2}{R_{eff}}\right)^2 + y^2} \tag{1}$$

$$\frac{1}{R_{eff}} = \frac{1}{2R_{lv}} + \frac{1}{2R_{br}} \tag{2}$$

where h_0 is the minimum spacing given by $h_0 = d_0 + 2a$, y is the lateral offset between the fibers as shown in Fig. 2. R_{eff} is the average radius of curvature of R_{lv} and R_{br} as illustrated in Fig. 3. When we choose a typical R_{lv} of 0.25 m, R_{eff} of the conventional symmetric structure ($R_{br} = 0.25$ m) is 0.25 m, while that of the asymmetric proposal is, as one example, $R_{br} = 0.5$ m yields R_{eff} of 0.33 m.

In the case of the phase-matched condition ($\Delta\beta = 0$), the through-transmission of uncoupled light η_{th} and cross-transmission η_{cr} can be calculated by [10]

$$\eta_{th} = \cos^2(c_0 L_{eff}) \tag{3}$$

$$\eta_{cr} = \sin^2(c_0 L_{eff}) \tag{4}$$

$$c_0 L_{eff} = \int_{-\infty}^{+\infty} c(z)dz, \tag{5}$$

where $c(z)$ is the coupling coefficient derived from [10]

$$c(z) = \frac{\lambda}{2\pi n_{co}} \frac{U^2}{a^2 V^2} \frac{K_0(Wh(z)/a)}{K_1^2(W)}, \tag{6}$$

where $c_0 = c(0)$, $y = 0$. Here, λ is the signal wavelength, n_{co} is the core refractive index, and K_i, are the modified Bessel functions

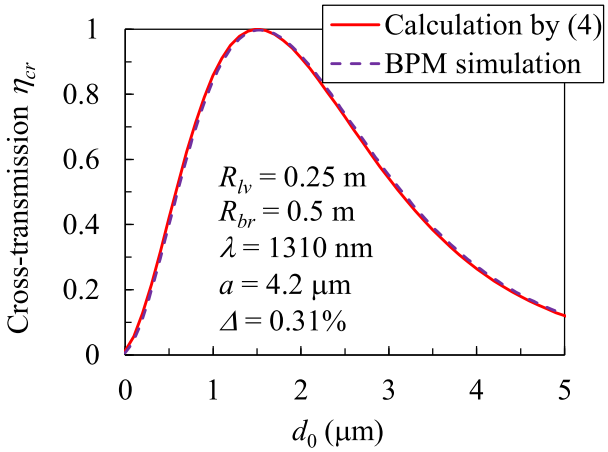

Fig. 4. Dependence of the cross-transmission on core distance d_0 calculated by (4) and BPM simulations.

of the second kind with order of i. V is the normalized frequency of the fiber at the signal wavelength given by

$$V = \frac{2\pi}{\lambda}\sqrt{n_{co}^2 - n_{cl}^2}, \tag{7}$$

where n_{cl} is the cladding refractive index. U and W are the transverse-mode parameters satisfying

$$U = \frac{2\pi}{\lambda}\sqrt{n_{co}^2 - n_{eff}^2},\ W = \frac{2\pi}{\lambda}\sqrt{n_{eff}^2 - n_{cl}^2} \tag{8}$$

where n_{eff} is the effective refractive index of the guided mode. L_{eff} is the effective interaction length given by

$$L_{eff} = \int_{-\infty}^{+\infty} \frac{K_0\left(Wh\left(z\right)/a\right)}{K_0\left(Wh_0/a\right)} dz. \tag{9}$$

The difference between our study and the conventional one [10] is R_{eff} in (1) and (2). Simply by using R_{eff}, the cross-transmission of the proposed asymmetric structure can be derived from (4) in the same way as the conventional symmetric one. Fig. 4 shows the dependence of the cross-transmission on the core distance d_0 as calculated by (4) and as simulated by the 3-D beam propagation method (BPM) with parameters of $a = 4.2$ μm, $\Delta = 0.31\%$, and $\lambda = 1310$ nm. In the BPM simulation, we simulated the asymmetric structure with $R_{lv} = 0.25$ m, $R_{br} = 0.5$ m as one example. The result calculated by (4) matches the BPM simulation result, which indicates that (1) and (2) are valid and useful for the design of asymmetric single-mode fiber couplers. Fig. 5 plots the maximum core distance d_0 for full-coupling as a function of R_{eff} at wavelengths of 1310, 1490, and 1550 nm. Although our goal is to decrease R_{lv} which triggers R_{eff} reduction, d_0 for full-coupling decreases as R_{eff} becomes small. We should set R_{eff} no smaller than 0.1 m so that d_0 for full-coupling does not become negative at a wavelength of 1310 nm. Fig. 6 shows the dependence of cross-transmission on core distance d_0 for various R_{br} in the case of $R_{lv} = 0.25$ m. d_0 for full-coupling of the asymmetric structure becomes wider than that of the symmetric one, which reduces the polishing loss by expanding d_{lv} [7]. For other than full-coupling, that is, $d_0 > 2$ μm, the asymmetric structure raises the highest

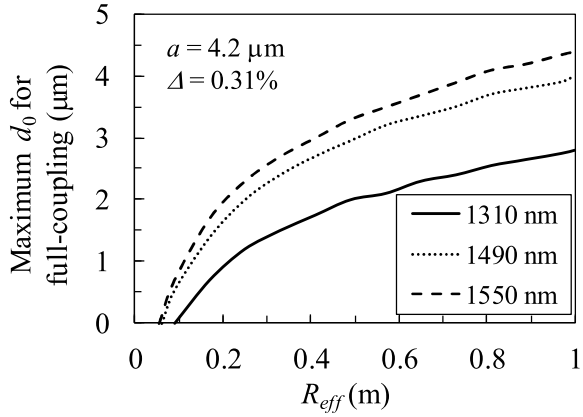

Fig. 5. Maximum core distance d_0 for full-coupling as a function of R_{eff}. Full-coupling is obtained when d_0 does not exceed the plots for each wavelength.

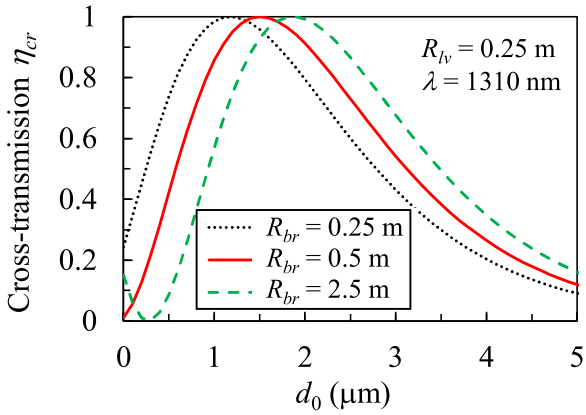

Fig. 6. Dependence of the cross-transmission on core distance d_0 for various R_{br} in the case of $R_{lv} = 0.25$ m.

cross-transmission by up to 0.13 for $d_0 = 2.4$ μm compared to the symmetric one. When we select $R_{br} = 2.5$ m [14], which is the largest radius yet reported to the best of our knowledge, the highest cross-transmission can be further improved by up to 0.26 for $d_0 = 2.4$ μm. Larger R_{br} yields higher cross-transmission but incurs higher costs as high-precision polishing machines are needed. R_{br} should be appropriately selected from 0.25 to 2.5 m according to the required cross-transmission value.

III. Fabrication of Side-Polished Fibers

We fabricated 13 side-polished fibers with R_{lv} of 0.25 m in the same way as [7]. A fabricated side-polished fiber is illustrated in Fig. 7. Their d_{lv} values can be estimated from the loss by polishing and the surface roughness because the polishing loss is considered to be scattering loss caused by roughness of the polished surface [7]. The surface roughness can be characterized by the following autocorrelation function $R(u)$ of the distribution function with zero mean $f(z)$ [20]

$$R\left(u\right) = \left\langle f(z)f(z+u)\right\rangle \approx \sigma^2 \exp\left(-\frac{|u|}{C}\right) \tag{10}$$

where the brackets represent the ensemble average, σ is the root-mean-square (RMS) roughness, and C is the correlation length.

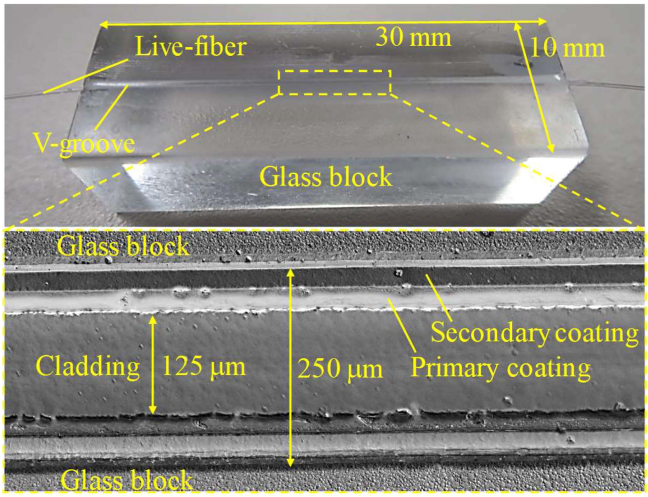

Fig. 7. Fabricated side-polished fiber. The live-fiber is held in a V-groove with radius of curvature of R_{lv} cut into the glass block.

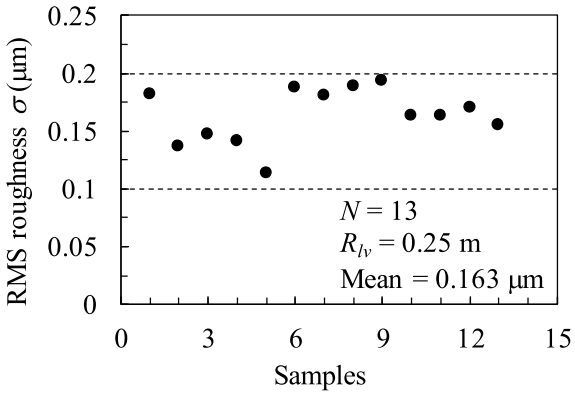

(a) RMS roughness σ

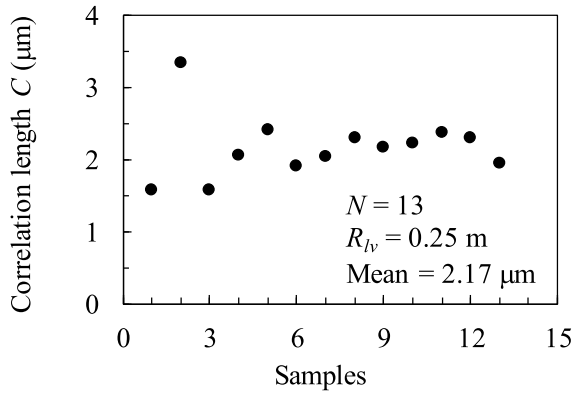

(b) Correlation length C

Fig. 8. Measured roughness of the polished surfaces by a laser confocal microscope.

Fig. 8 shows σ and C for the 13 samples measured by a laser confocal microscope (Keyence VK-X1000). We polished them using a commercially available optical connector polisher (NTT-AT ATP-3200) and a diamond polishing film with a particle size of 5 μm (NTT-AT AAS-DM05B). Purified water was applied to the polished surface before polishing to clean it and suppress

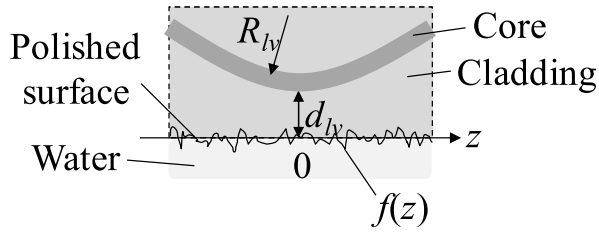

(a) Simulation model with the surface roughness.

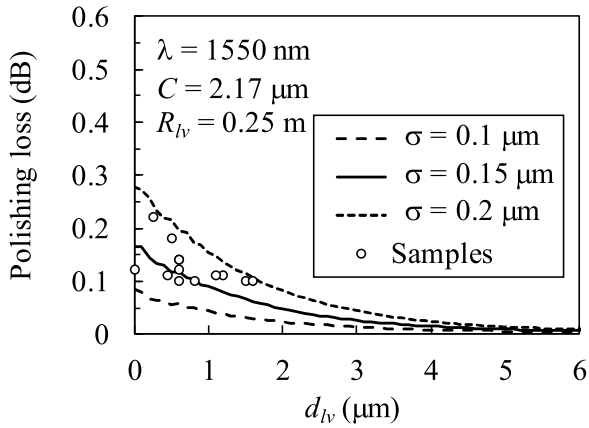

(b) Dependence of the polishing loss on d_{lv} for σ = 0.1, 0.15, and 0.2 μm.

Fig. 9. Polishing loss simulated with 3-D BPM and that of fabricated samples.

the temperature rise. The polishing pressure and speed were optimized so that polishing could be completed without breaking the fiber. The polishing was terminated when the polishing loss reached the target value of 0.1 to 0.22 dB to obtain various d_{lv}. The polishing took about 5 minutes on average. From Fig. 8, σ and C are distributed from 0.11 to 0.19 μm and from 1.6 to 3.3 μm, respectively. The roughness σ fluctuations are primarily caused by variations in the pressure per unit polishing area. The pressure variations are mainly due to the tilt of the polishing surface that occurs when the glass block with fixed optical fiber is set in the polishing machine. Tilting makes the pressure per unit polishing area stronger, which leads to a rougher polished surface. The correlation length C generally represents the extent of each irregularity on the polished surface and tends to be larger when there are relatively large polishing scratches or ridges. This is why the correlation length of sample 2 was larger than that of the other samples. Using these results, we calculated the dependence of the polishing loss on d_{lv} with the 3-D BPM by applying the roughness model satisfying (10) to the polished surface [7] as illustrated in Fig. 9(a). Fig. 9(b) represents the calculated dependence of the polishing loss on d_{lv} for $\sigma = 0.1$, 0.15, and 0.2 μm at the wavelength of 1550 nm. We chose a mean of $C = 2.17$ μm because the calculated result hardly changes even when C is changed from 1.6 to 3.3 μm. From Fig. 9(b), the polishing loss increases as d_{lv} decreases, but increases as σ increases. The estimated d_{lv} of the fabricated samples from the measured polishing loss and σ are also plotted in Fig. 9(b). The estimated d_{lv} ranges from 0 to 1.6 μm with a mean of 0.75 μm. This is mainly due to variation in roughness σ, which may be

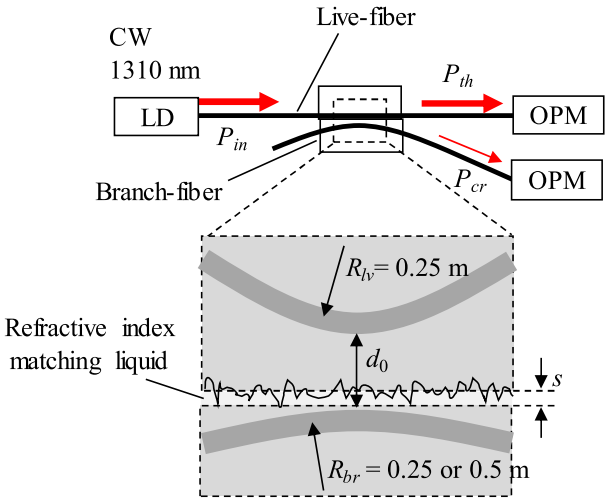

Fig. 10. Experimental setup. LD: Laser diode, OPM: Optical power meter.

reduced by optimizing the particle size of the polishing film and the polishing pressure.

IV. Results of the Experiment

We measured the cross-transmission, through-transmission, and excess loss with the experimental setup shown in Fig. 10. The branch-fiber can be assumed to be fabricated in the factory in advance and brought to the worksite. Accordingly, a stripped fiber with a diameter of 0.125 mm was precisely polished by using the liquid drop test [11], [12], [13] so that d_{br} was nearly zero. The branch-fibers that had R_{br} of 0.25 and 0.5 m were brought close to each sample of the side-polished live-fiber to compare the asymmetric structure with the symmetric one. The cross-transmission term η_{cr}, through-transmission η_{th}, and excess loss were calculated as follows.

$$\eta_{cr} = P_{cr}/P_{in} \tag{11}$$

$$\eta_{th} = P_{th}/P_{in} \tag{12}$$

$$ExcessLoss = 10\log_{10}\frac{P_{in}}{P_{th}+P_{cr}} \tag{13}$$

P_{in}, P_{th}, and P_{cr} are input power, output powers at the live- and branch-fiber, respectively, as shown in Fig. 10. Fig. 11 shows the experimental results when the live- and branch-fibers were aligned to obtain the highest cross-transmission at a wavelength of 1310 nm for R_{br} of 0.25 and 0.5 m. Fig. 11(a) confirmed that the highest cross-transmission of the asymmetric structure was raised by 0.15 on average compared to the symmetric one, which basically agrees with the calculated results in Fig. 6. On the other hand, there was some slight difference in the excess loss of both structures, see Fig. 11(c). It was experimentally revealed that the proposed asymmetric structure could improve the highest cross-transmission just by expanding R_{br} without changing R_{lv}. Higher through-transmission i.e., lower cross-transmission of sample 2 may be caused by relatively large polishing scratches or ridges as mentioned in Section III. The fluctuations of cross-transmission, through-transmission and excess loss among samples are mainly

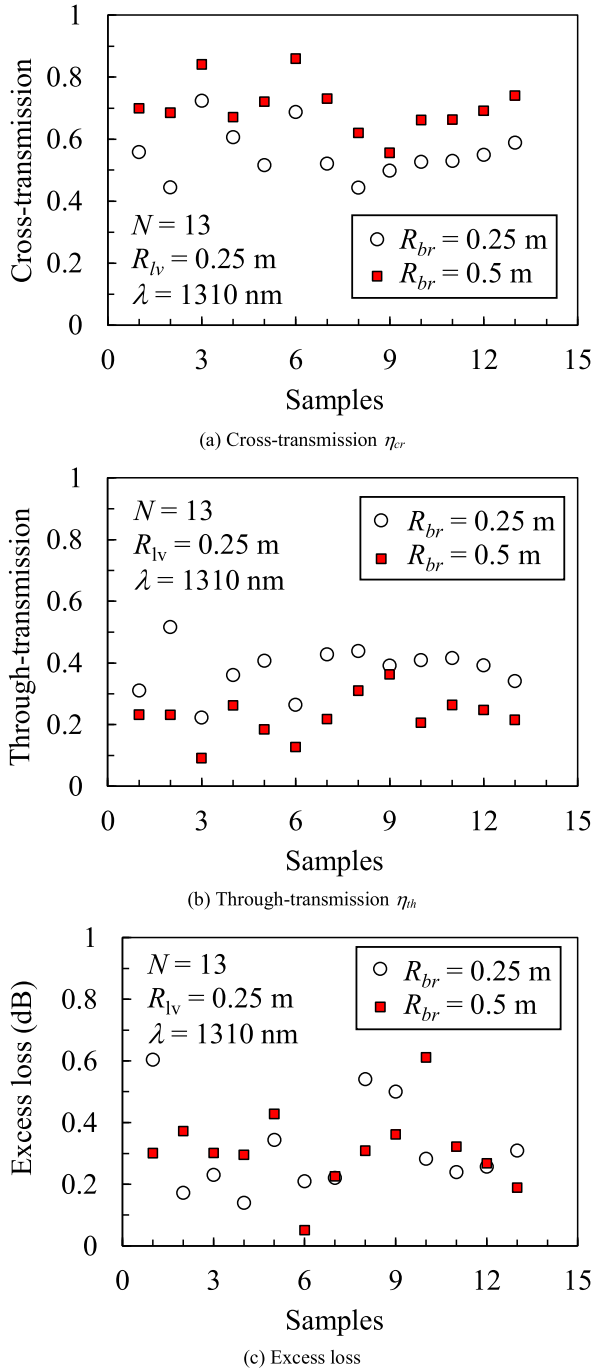

(a) Cross-transmission η_{cr}

(b) Through-transmission η_{th}

(c) Excess loss

Fig. 11. Experimental results when the live- and branch-fibers were aligned to maximize the cross-transmission at the wavelength of 1310 nm.

caused by variation in d_0, roughness, and flatness of the polished surfaces, which can be reduced by optimizing the particle size of the polishing film and the polishing pressure.

V. Discussion

Fig. 12 plots the core distance d_0 as estimated from the measured cross-transmission in Fig. 11(a), the measured excess loss in Fig. 11(c), and the dependence of cross-transmission on the core distance shown in Fig. 6. To remove the impact of excess

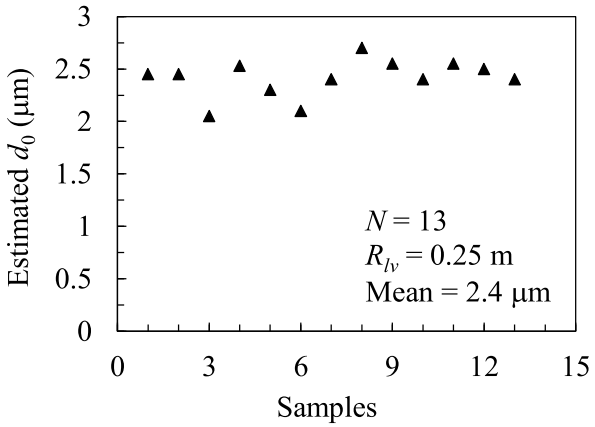

Fig. 12. Core distance d_0 estimated from the measured cross-transmission in Fig. 11(a), the excess loss in Fig. 11(c), and the dependence of cross-transmission on the core distance in Fig. 6.

loss from the estimation process, the highest branching ratio was obtained from

$$\eta'_{cr} = \frac{P_{cr}}{P_{th} + P_{cr}} \tag{14}$$

while estimated d_0 corresponding to η_{cr}' was derived from Fig. 6. The estimated d_0 ranged from 2.0 to 2.7 μm with a mean of 2.4 μm. Since d_{br} is nearly zero and the mean of the estimated d_{lv} was 0.75 μm as described in Fig. 9(b), the spacing between the polished surfaces s can be estimated to be about 1.65 μm. Although s can be reduced by improving the polishing precision such as using a polishing film with finer particle size and lower the polishing pressure, these approaches may lead to an increase in polishing time and size of the polishing machine, and so impair workability and portability. When $R_{br} = 2.5$ m, cross-transmission of about 0.9 can be obtained at a wavelength of 1310 nm for $d_0 = 2.4$ μm as indicated in Fig. 6.

VI. Conclusion

An asymmetric curvature side-polished fiber coupler composed of two side polished fibers with different curvature was proposed. In order to retain the convention curvature of the live-fiber while optimizing the optical properties of insertion loss and cross-transmission, the side-polished branch-fiber is given a relatively large curvature prior to installation in the field. We presented the (1) and (2) that simplified the calculation of the cross- and through- transmission for the design of the radii of curvature of the asymmetric single-mode fiber coupler. The BPM simulation revealed that the equations were valid. Our theoretical study showed that the proposed asymmetric structure could raise the highest cross-transmission by up to 0.26 without increasing the insertion loss. Experiments confirmed that the proposed structure improved the highest cross-transmission by 0.15 on average just by expanding R_{br} without changing R_{lv}. In addition, the results suggest that the highest cross-transmission of 0.9 can be realized by setting R_{lv} to the typical value of 0.25 m, with $R_{br} = 2.5$ m. Our study may contribute to realizing a simple and small polishing machine of live-fibers that offers enhanced workability and portability for the field installation of optical fiber couplers.

References

[1] *Gigabit-Capable Passive Optical Networks (GPON): General Characteristics*, Rec. ITU-T G. 984.1, International Telecommunications Union, Geneva, Switzerland, Mar. 2008.

[2] *IEEE Standard for Information Technology—Local and Metropolitan Area Networks—Part 3: CSMA/CD Access Method and Physical Layer Specifications Amendment: Media Access Control Parameters, Physical Layers, and Management Parameters for Subscriber Access Networks*, IEEE Standard 802.3ah-2004, pp. 1–640, Sep. 2004.

[3] R. N. Chiou, "Deploying FTTH with distributed control and bus topology," in *Proc. 16th Int. Conf. Adv. Commun. Technol.*, 2014, pp. 1178–1183.

[4] N. Bouabdallah, A.-L. Beylot, and E. Dotaro, "Resolving the fairness issues in bus-based optical access networks," *IEEE J. Sel. Areas Commun.*, vol. 23, no. 8, pp. 1444–1457, Aug. 2005.

[5] P. Lafata and J. Vodrazka, "Perspective application of passive optical network with optimized bus topology," *J. Appl. Res. Technol.*, vol. 10, no. 3, pp. 340–345, Jun. 2012.

[6] R. Igarashi et al., "Network design for bus-type optical access using distributed Raman amplification with asymmetric power splitter," *J. Lightw. Technol.*, vol. 39, no. 21, pp. 6814–6823, Nov. 2021.

[7] T. Uematsu, K. Noto, H. Iida, H. Hirota, and K. Katayama, "Optical coupling technique based on fiber side-polishing without service interruption," *IEEE Photon. Technol. Lett.*, vol. 34, no. 19, pp. 1042–1045, Oct. 2022.

[8] R. A. Bergh, G. Kotler, and H. J. Shaw, "Single-mode fiber optic directional coupler," *Electron. Lett.*, vol. 16, pp. 260–261, Mar. 1980.

[9] O. Parriaux, S. Gidon, and A. A. Kuznetsov, "Distributed coupling on polished single-mode optical fibers," *Appl. Opt.*, vol. 20, pp. 2420–2423, Jul. 1981.

[10] M. J. F. Digonnet and H. J. Shaw, "Analysis of a tunable single mode optical fiber coupler," *IEEE J. Quantum Electron.*, vol. 30, no. 4, pp. 746–754, Apr. 1982.

[11] M. J. F. Digonnet, J. R. Feth, and L. F. Stokes, "Measurement of the core proximity in polished fiber substrates and couplers," *Opt. Lett.*, vol. 10, no. 9, pp. 463–465, Sep. 1985.

[12] A. K. Das, M. A. Mondal, A. Mukherjee, and A. K. Mandal, "Automatic determination of the remaining cladding thickness of a single-mode fiber half-coupler," *Opt. Lett.*, vol. 19, no. 6, pp. 384–386, Mar. 1994.

[13] S.-M. Tseng and C.-L. Chen, "Side-polished fibers," *Appl. Opt.*, vol. 31, no. 18, pp. 3438–3447, Jun. 1992.

[14] S.-P. Ma and S.-M. Tseng, "High-performance side-polished fibers and applications as liquid crystal clad fiber polarizers," *J. Lightw. Technol.*, vol. 15, no. 8, pp. 1554–1558, Aug. 1997.

[15] J. Zhao et al., "Rough side-polished fiber with surface scratches for sensing applications," *IEEE Photon. J.*, vol. 7, no. 3, Jun. 2015, Art. no. 6801107.

[16] L. Zhuo et al., "High performance multifunction-in-one optoelectronic device by integrating graphene/MoS2 heterostructures on side-polished fiber," *Nanophotonics*, vol. 11, no. 6, pp. 1137–1147, Feb. 2022.

[17] L. Zhuo et al., "Side polished fiber: A versatile platform for compact fiber devices and sensors," *Photonic Sensors*, vol. 13, no. 1, Jun. 2022, Art. no. 230120.

[18] A. Grobelny, J. Witkowski, and E. Beres-Pawlik, "The numerical predictions of the parameters of asymmetrical couplers which pump double-clad lasers," in *Proc. Int. Conf. Transparent Opt. Netw.*, 2006, pp. 185–188.

[19] E. Beres-Pawlik and A. Grobelny, "Construction of a side pumped double-clad fiber using polished couplers," *Opt. Commun.*, vol. 283, no. 11, pp. 2363–2368, Feb. 2010.

[20] F. P. Payne and J. P. R. Lacey, "A theoretical analysis of scattering loss from planar optical waveguides," *Opt. Quantum Electron.*, vol. 26, no. 10, pp. 977–986, Oct. 1994.